NASA TECHNICAL NOTE

NASA TN D-5664

c. 1

NASA TN D-5664

NEWTON-RAPHSON—CONJUGATE-GRADIENT TECHNIQUE FOR CALCULATION OF AXISYMMETRIC BUCKLING OF SHALLOW SPHERICAL SHELLS WITH VARIABLE EDGE CONSTRAINT

by Harry G. Schaeffer

Langley Research Center
Langley Station, Hampton, Va.

NATIONAL AERONAUTICS AND SPACE ADMINISTRATION • WASHINGTON, D. C. • FEBRUARY 1970

1. Report No. NASA TN D-5664	2. Government Accession No.
3. Recipient's Catalog No.	
4. Title and Subtitle NEWTON-RAPHSON—CONJUGATE-GRADIENT TECHNIQUE FOR CALCULATION OF AXISYMMETRIC BUCKLING OF SHALLOW SPHERICAL SHELLS WITH VARIABLE EDGE CONSTRAINT	5. Report Date February 1970
	6. Performing Organization Code
7. Author(s) Harry G. Schaeffer	8. Performing Organization Report No. L-5959
9. Performing Organization Name and Address NASA Langley Research Center Hampton, Va. 23365	10. Work Unit No. 126-14-16-03-23
	11. Contract or Grant No.
12. Sponsoring Agency Name and Address National Aeronautics and Space Administration Washington, D.C. 20546	13. Type of Report and Period Covered Technical Note
	14. Sponsoring Agency Code

15. Supplementary Notes The information presented herein was included in a thesis entitled "The Direct Determination of Nonlinear Displacements of Arbitrarily Supported Shallow Shells Using Mathematical Programing Techniques" submitted in partial fulfillment of the requirements for the degree of Doctor of Philosophy in Engineering Mechanics, Virginia Polytechnic Institute, Blacksburg, Virginia, April 1967.

16. Abstract

The feasibility of utilizing mathematical programing techniques for determining stable equilibrium states of nonlinear structural systems is explored. The physical problem chosen for evaluation of this methodology was the nonlinear behavior of a shallow spherical shell subjected to uniform pressure. The procedure found most useful was a hybrid method consisting principally of a generalized Newton-Raphson technique with intermittent application of the conjugate-gradient search technique. The variation of buckling pressure with changes in edge restraint and shell geometry is found for a uniformly loaded shell.

17. Key Words Suggested by Author(s) Spherical shells; Buckling; Finite-difference approximations; Mathematical programing	18. Distribution Statement Unclassified – Unlimited

19. Security Classif. (of this report)	20. Security Classif. (of this page)	21. No. of Pages	22. Price*
Unclassified	Unclassified	30	$3.00

*For sale by the Clearinghouse for Federal Scientific and Technical Information
Springfield, Virginia 22151

NEWTON-RAPHSON—CONJUGATE-GRADIENT TECHNIQUE FOR CALCULATION OF AXISYMMETRIC BUCKLING OF SHALLOW SPHERICAL SHELLS WITH VARIABLE EDGE CONSTRAINT*

By Harry G. Schaeffer
Langley Research Center

SUMMARY

The feasibility of utilizing mathematical programing techniques for determining stable equilibrium states of nonlinear structural systems is explored. The physical problem chosen for evaluation of this methodology was the nonlinear behavior of a shallow spherical shell subjected to uniform pressure. The procedure found most useful was a hybrid method consisting principally of a generalized Newton-Raphson technique with intermittent application of the conjugate-gradient search technique. The variation of buckling pressure with changes in edge restraint and shell geometry is found for a uniformly loaded shell.

INTRODUCTION

In the areas of nonlinear mechanics and mathematical programing, significant progress has been made in the development of algorithms for minimizing a function of several variables. Typical of problems in nonlinear mechanics for which minimization procedures are particularly adaptable is the determination of stable axisymmetric equilibrium states of shallow spherical shells loaded by external pressure. This physical system exhibits the phenomenon of snap-buckling when a critical load is reached. The problem of a spherical shell with both clamped and simply supported edges has received a great deal of attention in recent years (refs. 1 to 11). References 3, 7, and 8 give clamped edge results, and reference 5 gives simply supported edge results. However, since no research has been directed toward shells with edge constraints between these

*The information presented herein was included in a thesis entitled "The Direct Determination of Nonlinear Displacements of Arbitrarily Supported Shallow Shells Using Mathematical Programing Techniques" submitted in partial fulfillment of the requirements for the degree of Doctor of Philosophy in Engineering Mechanics, Virginia Polytechnic Institute, Blacksburg, Virginia, April 1967.

two extremes, it would be of interest to investigate the buckling behavior for edge conditions which span these limits.

Variational procedures using a set of assumed functions, such as the Ritz technique (ref. 12), have been popular methods for obtaining approximate equilibrium states of both linear and nonlinear systems. In addition, several investigators (refs. 13 to 16) have shown that an appropriate set of finite-difference equations for linear conservative systems can be formulated by direct minimization of the energy function with respect to each unknown nodal displacement.

Nonlinear finite-difference equations are derived herein in a similar manner. The purpose of this report is to investigate the applicability of mathematical programing methods as a means of determining stable equilibrium states of nonlinear systems. The buckling result is an example of a difficult point to obtain. Several minimization algorithms are considered, and a hybrid method centered on the generalized Newton-Raphson procedure is used for calculations of buckling results for the spherical shell. New results are presented which show the variation of the buckling pressure of spherical shells with changes in edge constraint. In this study only axisymmetric buckling states are considered.

SYMBOLS

a	radius of curvature of spherical segment
b	radius from shell axis to edge of shell (see fig. 1)
D	bending stiffness, $\frac{Et^3}{12(1 - \nu^2)}$
d	nondimensional bending stiffness parameter, $\frac{1}{l^2}$
E	Young's modulus of elasticity
$e_r, e_\theta, e_{r\theta}$	middle surface strains
g_i	gradient of the potential function Π at x_i
H	maximum shell rise
h_j	assumed location of minimum of $\Pi(x)$

k	nondimensional membrane stiffness parameter, $12\left(\frac{b}{t}\right)^2$
k_r, k_θ	middle surface bending distortions
$\bar{l}$	reference length
l	nondimensional reference length, $\bar{l}/a$
N	number of real shell stations along a meridian (fig. 2)
n	number of unknowns
$\bar{p}$	dimensional surface pressure
p	nondimensional surface pressure, $\bar{p}/p_{cl}$
p_{cl}	classical buckling pressure defined in equation (5)
p_{cr}	axisymmetric buckling pressure corresponding to "top-of-the-knee" (point U in fig. 3)
q_1, q_2, q_3	boundary restraint coefficients (spring rates)
r	radius to shell middle surface from shell axis (see fig. 1)
s	scalar, optimum distance to proceed in direction v_i
t	shell thickness
$\bar{u}$	displacement along shell meridian
u	nondimensional meridional displacement, $\bar{u}/lb$
v_i	best direction to proceed from x_i^α (eq. (11))
$\bar{w}$	displacement normal to shell middle surface
w	nondimensional normal displacement, $\bar{w}/lb$

x	set of all x_i
x_i	set of all nodal displacements u_i, w_i
Δ	interval between shell stations, b/N
$\bar{\delta}$	preassigned small number (inequality (18))
δ_{ij}	Kronecker delta, $\delta_{ij} = 0$ for $i \neq j$; $\delta_{ij} = 1$ for $i = j$
$\epsilon_i, \epsilon_{i\pm(1/2)}$	integration factors evaluated at station i, and midway between station i and $i \pm 1$, respectively
$\epsilon_r, \epsilon_\theta$	strains
θ	circumferential coordinate
μ^2	geometric parameter for spherical shell, $\frac{\sqrt{12(1 - \nu^2)}\, b^2}{at}$
ν	Poisson's ratio
Π, Π_e, Π_s, Π_u	nondimensional total potential energy, edge force energy, surface force energy, strain energy, respectively
$\bar{\Pi}$	dimensional potential energy
Π_l, Π_{nl}	nondimensional linear and nonlinear components of Π, respectively
ρ	nondimensional radial coordinate, r/b
Ω	nondimensional surface pressure, $\frac{4}{l^2}\left(\frac{b}{a}\right)^2\left(\frac{b}{t}\right)p$
ω_1, ω_2	nondimensional curvatures; for spherical caps $\omega_1 = \omega_2 = \frac{b}{a}$

Superscripts:

α, β, γ	denote sequence number in iterative procedures

Primes indicate differentiation with respect to the nondimensional radial coordinate ρ.

POTENTIAL ENERGY FOR A SHALLOW SPHERICAL SHELL

The shell geometry is shown in figure 1. The shape is taken to be a shallow spherical cap. The shell has a thickness t and a spherical radius of curvature a. The displacements $\bar{u}$ and $\bar{w}$ are shown positive. The displacements $\bar{u}$ and $\bar{w}$ and the slope $\partial\bar{w}/\partial r$ may be elastically restrained at the shell boundary. The loading is an axisymmetric surface pressure $\bar{p}$ normal to the shell midsurface and positive outward. This pressure may vary along the meridian.

The total potential energy of the shell Π is composed of the strain energy Π_u, the energy of the external surface pressure Π_s, and the energy of boundary constraints Π_e:

$$\Pi = \Pi_u + \Pi_s + \Pi_e \tag{1}$$

In equation (1) the potential energy is nondimensional and a bar indicates a dimensional quantity where

$$\Pi = \frac{\overline{\Pi}}{\pi D l^2}$$

The strain energy for a shallow spherical cap is (ref. 17)

$$\Pi_u = \int_0^1 \left[k\left(e_r^2 + e_\theta^2 + 2\nu e_r e_\theta\right) + d\left(k_r^2 + k_\theta^2 + 2\nu k_r k_\theta\right)\right]\rho \, d\rho \tag{2}$$

where the strains and bending distortions are

$$\left.\begin{aligned}
e_r &= \omega_1 w + u' + \frac{1}{2}(w')^2 \\
e_\theta &= \omega_2 w - \frac{u}{\rho} \\
k_r &= -w'' \\
k_\theta &= \frac{-w'}{\rho}
\end{aligned}\right\} \tag{3}$$

and where the nondimensional radius, displacements, curvatures, and stiffnesses are given by

$$\rho = \frac{r}{b}$$

$$w = \frac{\bar{w}}{l b}$$

$$u = \frac{\bar{u}}{l b}$$

$$\omega_1 = \omega_2 = \frac{b}{a}$$

$$k = 12\left(\frac{b}{t}\right)^2$$

$$d = \frac{1}{l^2}$$

The potential energy for a uniform surface pressure $\bar{p}$ on the shell is

$$\Pi_S = -2\int_0^1 \Omega w\rho \, d\rho \tag{4}$$

where

$$\Omega = \frac{4}{l^2}\left(\frac{b}{a}\right)^2\left(\frac{b}{t}\right)p$$

and

$$p = \frac{\bar{p}}{p_{cl}}$$

The classical buckling pressure p_{cl} for a complete spherical shell is

$$p_{cl} = \frac{4Et}{a^2\sqrt{12(1 - \nu^2)}} \tag{5}$$

The potential energy for the arbitrary edge constraints (linear springs) integrated about the circumference at $\rho = 1$ is

$$\Pi_e = q_1 u_b^2 + q_2 w_b^2 + q_3\left(w_b'\right)^2 \tag{6}$$

where q_1, q_2, and q_3 are meridional, normal, and rotational nondimensional spring constants at the boundary. The subscript b denotes the subscripted quantity at the boundary $\rho = 1$.

The total potential energy from equations (1), (2), (4), and (6) is

$$\Pi = \int_0^1\Bigg(k\left\{\left[\omega_1 w + u' + \frac{1}{2}(w')^2\right]^2 + \left(\omega_2 w - \frac{u}{\rho}\right)^2 + 2\nu\left[\omega_1 w + u' + \frac{1}{2}(w')^2\right]\left(\omega_2 w - \frac{u}{\rho}\right)\right\}$$

$$+ d\left[(w'')^2 + \left(\frac{w'}{\rho}\right)^2 + \frac{2\nu w'' w'}{\rho}\right] - 2\Omega w\Bigg)\rho \, d\rho + q_1 u_b^2 + q_2 w_b^2 + q_3\left(w_b'\right)^2 \tag{7}$$

It is necessary to approximate equation (7) by a finite number of unknowns. This is accomplished in the present investigation by approximating the continuous functions (u,w) and the shell properties at N discrete stations along the meridian of the shell. These discrete stations are shown in figure 2. The radial interval between stations Δ is taken to be a constant, and the off-shell station $N + 1$ is added to allow the evaluation of derivatives at station N.

For convenience the numerical approximation of the potential function for the shallow spherical cap is written as

$$\Pi = \Pi_l + \Pi_{nl} \tag{8}$$

where Π_l involves terms in (u,w) of second degree and lower and Π_{nl} involves terms greater than second degree. Approximation of definite integrals by trapezoidal summations and the use of consistent numerical approximations for derivatives give the following expressions for Π_l and Π_{nl}:

$$\begin{aligned}\Pi_l = \sum_{i=1}^{N}\Bigg(\Bigg\{&k_{i-(1/2)}\left[u_{i-(1/2)}^2 + 2\left(\omega_1 + \nu\omega_2\right)w_{i-(1/2)}u'_{i-(1/2)} + \frac{2\nu u_{i-(1/2)}u'_{i-(1/2)}}{\rho_{i-(1/2)}}\right] \\ &+ \frac{d_{i-(1/2)}\left[w'_{i-(1/2)}\right]^2}{\rho_{i-(1/2)}}\Bigg\}\rho_{i-(1/2)}\epsilon_{i-(1/2)} + \Bigg\{k_i\Bigg[w_i^2\left(\omega_1^2 + \omega_2^2 + 2\nu\omega_1\omega_2\right) \\ &+ \frac{u_i^2}{\rho_i^2} + 2\left(\omega_2 + \nu\omega_1\right)\frac{w_i u_i}{\rho_i}\Bigg] + d_i\left[\left(w''_i\right)^2 + 2\nu\left(\frac{w'_i w''_i}{\rho_i}\right)\right] - 2\Omega_i w_i\Bigg\}\rho_i\epsilon_i\Bigg) + q_1 u_N^2 \\ &+ q_2 w_N^2 + q_3\left(w'_N\right)^2\end{aligned} \tag{9}$$

$$\Pi_{nl} = \sum_{i=1}^{N} k_{i-1}l\left\{\frac{l w_{i-(1/2)}^4}{4} + \left[w'_{i-(1/2)}\right]^2\left[\left(\omega_1 + \nu\omega_2\right)w_{i-(1/2)} + u'_{i-(1/2)} + \frac{\nu u_{i-(1/2)}}{\rho_{i-(1/2)}}\right]\right\}\rho_{i-(1/2)}\epsilon_{i-(1/2)} \tag{10}$$

An advantage of the potential-energy approach is that only geometric conditions are required at the pole, whereas procedures based on approximating the differential equations by finite differences require a shear condition also. These geometric conditions are imposed prior to minimizing the potential-energy function and require only that closure conditions specified at the pole insure finiteness of strain. Thus, the expressions for the circumferential midplane strain ϵ_θ and the midplane bending curvature k_θ (eqs. (3)) yield the conditions at $\rho = 0$, $u(0) = 0$, and $w'(0) = 0$.

FUNCTION MINIMIZATION

Computational Procedure

At this point it is necessary to set up an algorithm to perform the minimization of the energy (as given by eq. (8)), which may be identified as the object function Π. A computational procedure was chosen here on the basis that it might be applied to some general functional for many classes of problems involving a large number of variables where round-off error might be an important consideration and where maximums and inflection points may exist near the desired minimum.

Sequential search methods of minimization (refs. 18 to 27) were considered because such methods are quadratically convergent. The Newton-Raphson procedure, which utilizes both first and second derivatives, was considered and would have been used exclusively except that this method cannot be guaranteed always to tend toward a minimum. This deficiency will be discussed further in a subsequent section. The steepest-descent (ref. 20), variable-metric (refs. 24 and 25), and conjugate-gradient methods all appeared advantageous since only first derivatives of the object function were required. The steepest-descent method was ruled out since it is known to exhibit poor convergence characteristics for certain classes of problems (ref. 20). The variable-metric method requires storage and manipulation of a matrix and therefore is not suited to problems involving a large number of variables. The conjugate-gradient technique was the most advantageous method (after the Newton-Raphson procedure) but could not be used exclusively since the convergence characteristics of this method appear to be adversely affected by round-off error (see, also, refs. 21 and 26).

The linear axisymmetric behavior of a uniformly loaded circular plate was obtained in a sample calculation in which the plate was approximated by 22 unknowns. Since the potential function for this problem is quadratic, the conjugate-gradient method should converge in 22 iterations. For the plate example, however, approximately 400 iterations were required for single-precision calculations (8 digits) and 40 iterations for double-precision calculations (16 digits). This example shows the strong influence of round-off error on the results and ruled out the pure conjugate-gradient method for use in minimization of the potential function.

Thus, the minimization technique finally chosen was that of utilizing primarily the Newton-Raphson method but incorporating the conjugate-gradient method when the Newton-Raphson method failed to move toward a minimum point. This method, which will now be described in some detail, was used in this investigation to determine the buckling pressure of shallow spherical shells subjected to external pressure.

In both the Newton-Raphson and the conjugate-gradient methods, a new approximation of a dependent variable x is given in terms of the present approximation in the following form:

$$x_i^{\alpha+1} = x_i^{\alpha} + s^{\alpha} v_i^{\alpha} \tag{11}$$

where the superscript α denotes the iteration number.

The vector v_i^{α} represents the best direction to proceed from x_i^{α}, where x_i^{α} represents a point in an n-dimensional space and n is the number of unknowns. The scalar s^{α} represents an optimum distance to be traversed from x_i^{α} in the direction v_i^{α}. Here x_i is the set of all nodal variables associated with u and w. Equation (11) is to be used to generate a sequence of points x_i^1, x_i^2, . . ., x_i^{α}, $x_i^{\alpha+1}$ subject to the condition that

$$\Pi\left(x^{\alpha+1}\right) < \Pi\left(x^{\alpha}\right) \tag{12}$$

Newton-Raphson Procedure

The algorithm selected to perform the minimization was a generalized Newton-Raphson procedure (ref. 18). This method utilizes both first and second derivatives of the object function Π and assumes that $\Pi(x)$ and the first two derivatives are continuous. The use of this method for the expansion of $\Pi(x)$ at the point $x_i = x_i^{\alpha}$ leads to the following expression where terms higher than the second order are neglected:

$$\Pi(x) = \Pi\left(x^{\alpha}\right) + \frac{\partial \Pi\left(x^{\alpha}\right)}{\partial x_i}\left(x_i - x_i^{\alpha}\right) + \frac{1}{2}\,\frac{\partial^2 \Pi\left(x^{\alpha}\right)}{\partial x_i\,\partial x_j}\left(x_i - x_i^{\alpha}\right)\left(x_j - x_j^{\alpha}\right) \tag{13}$$

Since a necessary condition for a relative minimum is that the gradient of $\Pi(x)$ vanish, it follows that

$$\frac{\partial \Pi\left(x^{\alpha}\right)}{\partial x_i} + \frac{\partial^2 \Pi\left(x^{\alpha}\right)}{\partial x_i\,\partial x_j}\, e_j^{\alpha} = 0 \tag{14}$$

where terms greater than the first degree in x_i have been dropped and where

$$e_j^{\alpha} = h_j^{\alpha} - x_j^{\alpha} \tag{15}$$

is the error vector corresponding to the difference between the minimum point h_j^{α} and x_j^{α}. Since the quanties $\frac{\partial \Pi}{\partial x_i}$ and $\frac{\partial^2 \Pi}{\partial x_i\,\partial x_j}$ are known at x_j^{α}, the error vector e_j^{α} can be found by the matrix inverse as follows:

$$e_j^{\alpha} = -\left[\frac{\partial^2 \Pi\left(x^{\alpha}\right)}{\partial x_i\,\partial x_j}\right]^{-1} \frac{\partial \Pi\left(x^{\alpha}\right)}{\partial x_i} \tag{16}$$

The derivative terms on the right-hand side of equation (16) are presented for the object function Π as given in the appendix. For this problem the matrix to be inverted on the right-hand side of equation (16) is symmetric and has a narrow band of nonzero terms. The error vector e_j^α is therefore obtained conveniently from equation (14) using Gaussian elimination.

Once the error vector e_j^α is calculated, then the new approximation becomes

$$x_j^{\alpha+1} = x_j^\alpha + e_j^\alpha \tag{17}$$

This sequence of calculations (eqs. (16) and (17)) is repeated until

$$\left\| e_j^\alpha \right\| < \bar{\delta} \left\| x^\alpha \right\| \tag{18}$$

where $\bar{\delta}$ is a preassigned small number. When inequality (18) is satisfied, then the procedure has presumably converged to the solution h_j where

$$h_j = x_j^{\alpha+1}$$

The generalized Newton-Raphson procedure has a drawback in that inequality (12) is not necessarily satisfied. The solution may tend toward a maximum or stationary point rather than a minimum. A check is made after each iteration to insure that inequality (12) has been satisfied. When the test fails and inequality (12) is not satisfied, then a new starting point which guarantees a move toward a minimum is required. A conjugate-gradient technique was selected for the restart toward a minimum.

Restart by Conjugate-Gradient Method

Assume that at some iteration number $(\beta + 1)$ the inequality (12) is not satisfied and that x_i^β is the last approximation satisfying the inequality (12). By the conjugate-gradient method (refs. 20 to 23) the unknown vector v_i^β, required in equation (11), is given by

$$v_i^\beta = -\frac{\partial \Pi\left(x_i^\beta\right)}{\partial x_i^\beta} \tag{19}$$

The distance s^β in the direction v_i^β is given by

$$\frac{\partial \Pi}{\partial s^\beta}\left(x_i^\beta + s^\beta v_i^\beta\right) = 0 \tag{20}$$

From equation (11),

$$x_i^{\beta+1} = x_i^\beta + s^\beta v_i^\beta \tag{21}$$

For subsequent iterations by this method,

$$v_i^\gamma = -g_i^\gamma + \frac{g_i^\gamma \cdot g_i^\gamma}{g_i^{\gamma-1} \cdot g_i^{\gamma-1}} v_i^{\gamma-1} \tag{22}$$

where

$$g_i^\gamma = \frac{\partial \Pi\left(x_i^\gamma\right)}{\partial x_i^\gamma}$$

and s^γ is given by equation (20) with β replaced by γ. Each iteration leads to a new approximation $x_i^{\gamma+1}$ from equation (11).

Only a few cycles are usually required to satisfy inequality (12), and then the Newton-Raphson procedure can be resumed.

APPLICATION TO BUCKLING OF SPHERICAL SHELL

The pressure-deflection curve for a uniformly loaded shallow shell has the general form shown in figure 3 (see, e.g., ref. 8). The buckling pressure p_{cr} is defined as the pressure corresponding to point U on the curve. This curve OULN is representative of those shells for which $\mu^2 > 11$, where μ^2 is defined as

$$\mu^2 = \sqrt{12\left(1 - \nu^2\right)}\left(\frac{b^2}{at}\right)$$

Very shallow shells $\left(\mu^2 < 11\right)$ are of no interest since the curve OULN increases monotonically and there is no definable top-of-the-knee.

In the prebuckled range, the Newton-Raphson procedure converges rapidly when the linear solution is used as the initial-state point. In the region of interest for buckling pressures, that is, near point U, convergence difficulties may occur when the Newton-Raphson procedure alone is used and when the most recent converged-state point or the linear solution is used as an initial state. For pressures greater than that associated with point U with a similar assumed initial state, the Newton-Raphson procedure will not converge. In the region of interest approaching point U a restart by the conjugate-gradient method needs to be applied.

Two convergence tests are made in the application of the Newton-Raphson procedure. The first (inequality (12)) determines that the function is being minimized and the second (inequality (18)) determines the location of the minimum to an acceptable degree of accuracy. In this study $\bar{\delta}$ was taken as 0.05.

If inequality (12) is not satisfied after a prescribed number of restarts of the Newton-Raphson—conjugate-gradient procedure, the pressure increment is reduced and the procedure is again applied. If two successive reductions of the pressure increment do not lead to convergence, by satisfying inequality (12), then it is assumed that the pressure associated with the last converged result is the buckling pressure. In the present investigation the new pressure increment is taken as 1/5 of the current pressure increment so that the buckling pressure is found to within $0.025\Delta p$, where Δp is the magnitude of the pressure increment. When the Newton-Raphson procedure is reinitiated after reducing the pressure increment, the last converged solution is used as an initial approximation of the location of the minimum.

EFFECT OF EDGE CONSTRAINTS ON THE AXISYMMETRIC BUCKLING OF A SPHERICAL SHELL

The minimization procedure and resulting computer program were used to study the influence of arbitrary edge constraints on the axisymmetric buckling pressure of a spherical cap. Comparisons are made between present results and those of previous investigators. For the present investigation, 10 finite-difference increments were used along a shell meridian together with the following parameter values:

$$\nu^2 = 0.1$$

$$b/t = 100$$

$$q_2 = 10^5$$

where the value of q_2 is essentially large enough to constrain normal edge displacement.

The variation of the axisymmetric buckling pressure with shell parameter μ for clamped and simply supported edges was obtained for comparison with results presented by other investigators as an evaluation of the minimization procedure. (For example, see ref. 8 for clamped results and ref. 28 for simply supported results.) The results are shown in figure 4 where it is seen that buckling pressures as determined by the procedure are in good agreement with the results of the two references indicated by the solid symbols. The slight variations may be due to differences in finite-difference spacings and other approximations in the various numerical procedures. Here the values of the rotational spring constant q_3 was taken as 10^5 to approximate completely constrained edge rotation and as 0 for the simply supported edge.

Meridional Edge Restraint

Results were also obtained for variations in meridional restraint as well as rotational restraints. Results were limited to values of $\mu \leqq 6$ since it has been shown that for $\mu > 6$, asymmetric buckling governs (ref. 29). To determine the influence of meridional restraint on the buckling behavior of shallow spherical shells, plots of the buckling pressure p_{cr} for various values of the in-plane restraint parameter q_1 are shown in figure 5 for geometric shell parameters μ of 4, 5, and 6. The calculations were carried out for a shallow spherical cap with the edge essentially fully restrained against rotation $(q_3 = 10^5)$. The plots show that the buckling pressure is essentially insensitive to the in-plane restraint at the extreme regions of meridional restraint $(q_1 < 10^3$ and $q_1 > 10^7)$. Between these extremes the buckling pressure increases monotonically with an increase in in-plane restraint.

From the above results an estimate can be made of the size of an edge ring of solid circular cross section which would be required to approximate a rigid restraint to meridional displacement. By assuming that $q_1 = 10^7$ and that the ring and shell are made of the same material, it is found that a relatively large ring cross-sectional radius of approximately 50t is required, where t is the thickness of the shell.

Rotational Edge Restraint

Calculations were also made to determine the influence of rotational restraint on the buckling behavior of shallow spherical shells. Plots of the buckling pressure p_{cr} for various values of the rotational restraint parameter q_3 are shown in figure 6 for geometric parameters μ of 4, 5, and 6. The calculations were carried out for a shallow spherical cap with the meridional edge displacement essentially fully restrained $(q_1 = 10^7)$. The plots show that the buckling pressure is essentially insensitive to the rotational restraint for the extreme regions of plot $(q_3 < 0.01$ and $q_3 > 10^3)$. Between these extremes the character of the variation of buckling pressure with a change in the rotational restraint parameter is dependent on the value of the geometric shell parameter μ.

Figure 6 shows two effects which are of interest. First, that for $\mu = 5$ and 6 a peak in the p_{cr} curve occurs between the extremes of edge conditions, that is, clamped $(q_3 > 10^3)$ and simply supported $(q_3 < 0.01)$. Second, that for $\mu = 4$ and 5 the buckling pressure for the simply supported edge condition is greater than the buckling pressure for the clamped edge condition. Although the first effect was unexpected, it can be correlated to some degree with changes in the normal deflection mode shapes. The mode shapes just prior to buckling were calculated for several combinations of the parameters. The results are shown in figures 7(a), 7(b), and 7(c) for geometric shell parameters μ of 4, 5, and 6, respectively, and for values of the rotational restraint parameter q_3 associated with the simply supported and clamped edge conditions. In figures 7(b) and 7(c), the modes associated with values of the rotational restraint parameter just prior to and just after the peak in p_{cr} are also included. It is seen that the simply supported $\left(q_3 = 0\right)$ buckling mode changes between $\mu = 4$ and $\mu = 5$ and that the clamped $\left(q_3 \approx 10^5\right)$ buckling mode changes between $\mu = 5$ and $\mu = 6$.

With regard to the second effect shown in figure 6, other investigators have noted that the spherical shell with a simply supported edge has a higher buckling pressure than the same shell with a clamped edge (e.g., ref. 30). The increase in buckling pressure was attributed to dynamic effects in reference 30, whereas the results of the present investigation show that the increase occurs statically and is associated with the buckling mode. Perhaps in this range the buckling pressure for the simply supported edge would be lower than for the clamped edge if asymmetric buckling were included in the study.

The explanation for the peak in the variation in buckling pressure with rotational restraint is not apparent. It does appear, however, that the results are not unreasonable in view of the variation of buckling pressure with μ shown in figure 4. The very sharp peak shown in figure 6 for $\mu = 5$ is evidently related to the fact that the mode shape for the clamped edge has one half-wave whereas the mode shape for the simply supported edge has the character of 3 half-waves.

The size of an edge ring of solid circular cross section required to approximate a rigid rotational restraint $\left(q_3 > 10^3\right)$ has been calculated. A ring radius of approximately 10t is equivalent to $q_3 = 10^3$, where the ring and shell are made of the same material. This is considerably smaller than the ring radius of approximately 50t required to simulate a rigid restraint to meridional displacement. Thus, in the design of a supporting ring to simulate clamped edge conditions, the meridional restraint is the controlling factor.

CONCLUDING REMARKS

A direct minimization of an object function was used to demonstrate that for nonlinear static structural problems, stable equilibrium states can be determined numerically. The method developed was applied to determine the "top-of-the-knee" buckling pressures of shallow spherical shells with various edge restraints. In this case the object function was the potential energy of the system.

Several mathematical programing techniques were evaluated. These techniques included steepest-descent, conjugate-gradient, variable-metric and generalized Newton-Raphson methods. It was found that the procedure most appropriate for this class of problems is a hybrid method composed primarily of a generalized Newton-Raphson procedure with selected applications of the conjugate-gradient method.

This computational procedure was chosen here on the basis that it might be applied to some general functional for many classes of problems involving a large number of variables where round-off error might be an important consideration and where maximum and inflection points may exist near the desired minimum.

The procedure has been used to study the influences of a wide range of rotational and meridional boundary restraint on the axisymmetric buckling of a shallow spherical cap subjected to a uniformly distributed pressure. The variations of buckling pressure with changes in in-plane and rotational edge restraint for uniformly loaded shells for several values of the geometric shell parameter μ show that for $\mu \geqq 5$, partial rotational restraint can yield higher buckling pressures than for either clamped or simply supported edges. It was also found that a very large value of meridional in-plane stiffness was required in order to approach the greater strength corresponding to the completely restrained condition.

Langley Research Center,
National Aeronautics and Space Administration,
Langley Station, Hampton, Va., December 4, 1969.

APPENDIX

DERIVATIVES OF SHALLOW-SHELL POTENTIAL FUNCTION

The first and second derivatives of the potential function, equation (8), which are required in the Newton-Raphson minimization procedure are found by differentiation of the potential with respect to the nodal displacements.

Gradients

Differentiation of the linear potential Π_l with respect to u_i and w_i leads to the following gradient components:

$$
\begin{aligned}
\frac{\partial \Pi_l}{\partial w_i} = {} & \epsilon_{i+(1/2)}\rho_{i+(1/2)}\left\{k_{i+(1/2)}\left[u'_{i+(1/2)}\left(\omega_1 + \nu\omega_2\right)_{i+(1/2)}\right] + 2\,\frac{d_{i+(1/2)}}{\rho^2_{i+(1/2)}}\,w'_{i+(1/2)}\left(-\frac{1}{\Delta}\right)\right\} \\
& + \epsilon_{i-(1/2)}\rho_{i-(1/2)}\left\{k_{i-(1/2)}\left[u'_{i-(1/2)}\left(\omega_1 + \nu\omega_2\right)_{i-(1/2)}\right] + 2\,\frac{d_{i-(1/2)}}{\rho^2_{i-(1/2)}}\,w'_{i-(1/2)}\left(\frac{1}{\Delta}\right)\right\} \\
& + \epsilon_i\rho_i\left\{b_i\left[2w_i\left(\omega_1^2 + \omega_2^2 + 2\nu\omega_1\omega_2\right)_i + 2\,\frac{u_i}{\rho_i}\left(\omega_2 + \nu\omega_1\right)_i\right] + d_i\left[2w''_i\left(-\frac{2}{\Delta^2}\right) + \frac{2\nu}{\rho_i}\,w'_i\left(-\frac{2}{\Delta^2}\right)\right]\right. \\
& \left. - 2\Omega_i\right\} + \epsilon_{i+1}\rho_{i+1}d_{i+1}\left[2w''_{i+1}\left(\frac{1}{\Delta^2}\right) + \frac{2\nu}{\rho_{i+1}}\left(-\frac{w''_{i+1}}{2\Delta} + \frac{w'_{i+1}}{\Delta^2}\right)\right] + \epsilon_{i-1}\rho_{i-1}d_{i-1}\left[2w''_{i-1}\left(\frac{1}{\Delta^2}\right)\right. \\
& \left. + \frac{2\nu}{\rho_{i-1}}\left(\frac{w''_{i-1}}{2\Delta} + \frac{w'_{i-1}}{\Delta^2}\right)\right] + 2q_2 w_{N-1}\delta_{i,N-1} + \frac{q_3}{\Delta}\left(w_N\delta_{i,N} - w_{N-2}\delta_{i,N-2}\right)
\end{aligned}
$$

$$(i = 1, 2, \ldots, N + 1) \qquad \textbf{(A1)}$$

$$
\begin{aligned}
\frac{\partial \Pi_l}{\partial u_i} = {} & \epsilon_{i+(1/2)}\rho_{i+(1/2)}k_{i+(1/2)}\left\{2u'_{i+(1/2)}\left(-\frac{1}{\Delta}\right) + 2w_{i+(1/2)}\left(-\frac{1}{\Delta}\right)\left(\omega_1 + \nu\omega_2\right)_{i+(1/2)}\right. \\
& \left. + \frac{2\nu}{\rho_{i+(1/2)}}\left[u_{i+(1/2)}\left(-\frac{1}{\Delta}\right)u'_{i+(1/2)}\left(\frac{1}{2}\right)\right]\right\} + \epsilon_{i-(1/2)}\rho_{i-(1/2)}k_{i-(1/2)}\left\{2u'_{i-(1/2)}\left(\frac{1}{\Delta}\right)\right. \\
& \left. + 2w_{i-(1/2)}\left(\frac{1}{\Delta}\right)\left(\omega_1 + \nu\omega_2\right)_{i-(1/2)} + \frac{2\nu}{\rho_{i-(1/2)}}\left[u_{i-(1/2)}\left(\frac{1}{\Delta}\right) + \frac{1}{2}\,u'_{i-(1/2)}\right]\right\} + \epsilon_i k_i\rho_i\left[2\,\frac{u_i}{\rho_i^2}\right. \\
& \left. + 2\,\frac{w_i}{\rho_i}\left(\omega_2 + \nu\omega_1\right)_i\right] + 2q_1 u_{N-1}\delta_{i,N-1} \qquad (i = 1, 2, \ldots, N + 1) \qquad \textbf{(A2)}
\end{aligned}
$$

where ϵ_i and $\epsilon_{i+(1/2)}$ are integrating factors having values as follows:

$$\epsilon_{N+(1/2)} = 0$$

$$\epsilon_{i+(1/2)} = \Delta \qquad (i = 1, 2, \ldots, N)$$

$$\epsilon_i = \Delta \qquad (i = 2, 3, \ldots, N - 1)$$

$$\epsilon_1 = 0$$

$$\epsilon_{N+1} = 0$$

$$\epsilon_N = \frac{\Delta}{2}$$

and N is the number of stations on the shell. An off-shell station N + 1 is considered so that the derivative of (u,w) may be evaluated at the edge. The quantity δ_{ij} is the Kronecker delta and is defined as follows:

$$\delta_{ij} = \begin{cases} 0 & (i \neq j) \\ 1 & (i = j) \end{cases}$$

In a similar manner contribution of the nonlinear potential to the gradient components is as follows:

$$\begin{aligned} \frac{\partial \Pi_{nl}}{\partial w_i} = {} & k_{i+(1/2)}\rho_{i+(1/2)}\epsilon_{i+(1/2)}l\left\{l\left(w'\right)^3_{i+(1/2)}\left(-\frac{1}{\Delta}\right) + 2w'_{i+(1/2)}\left(-\frac{1}{\Delta}\right)\left[w_{i+(1/2)}\left(\omega_1 + \nu\omega_2\right)_{i+(1/2)}\right.\right. \\ & \left.\left. + u'_{i+(1/2)} + \nu\frac{u_{i+(1/2)}}{\rho_{i+(1/2)}}\right] + \frac{\left(w'\right)^2_{i+(1/2)}}{2}\left(\omega_1 + \nu\omega_2\right)_{i+(1/2)}\right\} \\ & + k_{i-(1/2)}\rho_{i-(1/2)}\epsilon_{i-(1/2)}l\left\{l\left(w'\right)^3_{i-(1/2)}\left(\frac{1}{\Delta}\right) + 2w_{i-(1/2)}\left(\frac{1}{\Delta}\right)\left[w_{i-(1/2)}\left(\omega_1 + \nu\omega_2\right)_{i-(1/2)}\right.\right. \\ & \left.\left. + u'_{i-(1/2)} + \nu\frac{u_{i-(1/2)}}{\rho_{i-(1/2)}}\right] + \frac{\left(w'\right)^2_{i-(1/2)}}{2}\left(\omega_1 + \nu\omega_2\right)_{i-(1/2)}\right\} \end{aligned} \tag{A3}$$

$$\frac{\partial\Pi_{N1}}{\partial u_i} = k_{i+(1/2)}\rho_{i+(1/2)}\epsilon_{i+(1/2)}l\left\{(w')^2_{i+(1/2)}\left[-\frac{1}{\Delta} + \frac{\nu}{2\rho_{i+(1/2)}}\right]\right\}$$

$$+ k_{i-(1/2)}\rho_{i-(1/2)}\epsilon_{i-(1/2)}l\left\{(w')^2_{i-(1/2)}\left[\frac{1}{\Delta} + \frac{\nu}{2\rho_{i-(1/2)}}\right]\right\} \tag{A4}$$

where $i = 1, 2, \ldots, N + 1$.

Second Derivative of the Potential Function

The differentiation of the gradient components with respect to nodal displacements leads to the following expressions for second derivatives of Π_1:

$$\frac{\partial^2\Pi_1}{\partial w_i^2} = \frac{2\bar{d}_{i+(1/2)}}{\Delta^2\rho^2_{i+(1/2)}} + \frac{2\bar{d}_{i-(1/2)}}{\Delta^2\rho^2_{i-(1/2)}} + 2\bar{k}_i\left(\omega_1^2 + \omega_2^2 + 2\nu\omega_1\omega_2\right)_i + \frac{8\bar{d}_i}{\Delta^4} + \bar{d}_{i+1}\left(\frac{2}{\Delta^4} - \frac{2\nu}{\rho_{i+1}\Delta^3}\right)$$

$$+ \bar{d}_{i-1}\left(\frac{2}{\Delta^4} + \frac{2\nu}{\rho_{i-1}\Delta^3}\right) + 2\bar{q}_3\delta_{i,N-1} + \frac{\bar{q}_4}{\Delta}\left(\delta_{i,N} - \delta_{i,N-2}\right) \tag{A5}$$

$$\frac{\partial^2\Pi_1}{\partial w_i\,\partial w_{i-1}} = \bar{d}_i\left(-\frac{4}{\Delta^4} + \frac{2\nu}{\rho_i\Delta^3}\right) - \frac{2\bar{d}_{i-(1/2)}}{\rho^2_{i-(1/2)}\Delta^2} - \bar{d}_{i-1}\left(\frac{4}{\Delta^4} + \frac{2\nu}{\rho_{i-1}\Delta^3}\right) \tag{A6}$$

$$\frac{\partial^2\Pi_1}{\partial w_i\,\partial w_{i+1}} = -\bar{d}_i\left(\frac{4}{\Delta^4} + \frac{2\nu}{\rho_i\Delta^3}\right) - \frac{2\bar{d}_{i+(1/2)}}{\rho^2_{i+(1/2)}\Delta^2} + \bar{d}_{i+1}\left(-\frac{4}{\Delta^4} + \frac{2\nu}{\rho_{i+1}\Delta^3}\right) \tag{A7}$$

$$\frac{\partial^2\Pi_1}{\partial w_i\,\partial w_{i-2}} = \frac{2\bar{d}_{i-1}}{\Delta^4} \tag{A8}$$

$$\frac{\partial^2\Pi_1}{\partial w_i\,\partial w_{i+2}} = \frac{2\bar{d}_{i+1}}{\Delta^4} \tag{A9}$$

$$\frac{\partial^2\Pi_1}{\partial w_i\,\partial u_i} = -\bar{k}_{i+(1/2)}\frac{\left(\omega_1 + \nu\omega_2\right)_{i+(1/2)}}{\Delta} + \bar{k}_{i-(1/2)}\frac{\left(\omega_1 + \nu\omega_2\right)_{i-(1/2)}}{\Delta} + \frac{2\bar{k}_i}{\rho_i}\left(\omega_2 + \nu\omega_1\right)_i \tag{A10}$$

$$\frac{\partial^2 \Pi_l}{\partial u_i \; \partial w_{i-1}} = \bar{k}_{i-(1/2)} \frac{\left(\omega_1 + \nu\omega_2\right)_{i-(1/2)}}{\Delta} \tag{A11}$$

$$\frac{\partial^2 \Pi_l}{\partial u_i \; \partial w_{i+1}} = -\bar{k}_{i+(1/2)} \frac{\left(\omega_1 + \nu\omega_2\right)_{i+(1/2)}}{\Delta} \tag{A12}$$

$$\frac{\partial^2 \Pi_l}{\partial u_i^2} = \bar{k}_{i+(1/2)}\left[\frac{2}{\Delta^2} - \frac{2\nu}{\rho_{i+(1/2)}\Delta}\right] + \bar{k}_{i-(1/2)}\left[\frac{2}{\Delta^2} + \frac{2\nu}{\rho_{i-(1/2)}\Delta}\right] + \frac{2\bar{k}_i}{\rho_i^2} + 2q_i\delta_{i,N-1} \tag{A13}$$

$$\frac{\partial^2 \Pi_l}{\partial u_i \; \partial u_{i-1}} = -\frac{2\bar{k}_{i-(1/2)}}{\Delta^2} \tag{A14}$$

$$\frac{\partial^2 \Pi_l}{\partial u_i \; \partial u_{i+1}} = -\frac{2\bar{k}_{i+(1/2)}}{\Delta^2} \tag{A15}$$

where

$$\bar{k}_i = k_i\rho_i\epsilon_i$$

$$\bar{d}_i = d_i\rho_i\epsilon_i$$

Similarly, the second derivatives of the nonlinear potential Π_{nl} are as follows:

$$\begin{aligned}\frac{\partial^2 \Pi_{nl}}{\partial w_i^2} = \bar{k}_{i+(1/2)}\Bigg\{3l\left(w'\right)^2_{i+(1/2)}\left(\frac{1}{\Delta}\right)^2 &+ \frac{2}{\Delta^2}\left[w_{i+(1/2)}\left(\omega_1 + \nu\omega_2\right)_{i+(1/2)} + u'_{i+(1/2)} + \frac{\nu u_{i+(1/2)}}{\rho_{i+(1/2)}}\right] \\ &- \frac{2}{\Delta} w'_{i+(1/2)}\left(\omega_1 + \nu\omega_2\right)_{i+(1/2)}\Bigg\} - \bar{k}_{i-(1/2)}\Bigg\{3l\left(w'\right)^2_{i-(1/2)}\left(\frac{1}{\Delta^2}\right) \\ &+ \frac{2}{\Delta^2}\left[w_{i-(1/2)}\left(\omega_1 + \nu\omega_2\right)_{i-(1/2)} + u'_{i-(1/2)} + \frac{\nu u_{i-(1/2)}}{\rho_{i-(1/2)}}\right] \\ &+ \frac{2}{\Delta} w'_{i-(1/2)}\left(\omega_1 + \nu\omega_2\right)_{i-(1/2)}\Bigg\}\end{aligned} \tag{A16}$$

$$\frac{\partial^2 \Pi_{nl}}{\partial w_i \ \partial w_{i-1}} = \bar{k}_{i-1}\left\{-\frac{3l}{\Delta^2}(w')^2_{i-(1/2)} - \frac{2}{\Delta^2}\left[w_{i-(1/2)}(\omega_1 + \nu\omega_2)_{i-(1/2)} + u'_{i-(1/2)} + \frac{\nu u_{i-(1/2)}}{\rho_{i-(1/2)}}\right]\right\} \tag{A17}$$

$$\frac{\partial^2 \Pi_{nl}}{\partial w_i \ \partial w_{i+1}} = \bar{k}_{i+1}\left\{-\frac{3l}{\Delta^2}(w')^2_{i+(1/2)} - \frac{2}{\Delta^2}\left[w_{i+(1/2)}(\omega_1 + \nu\omega_2)_{i+(1/2)} + u'_{i+(1/2)} + \frac{\nu u_{i+(1/2)}}{\rho_{i+(1/2)}}\right]\right\} \tag{A18}$$

$$\frac{\partial^2 \Pi_{nl}}{\partial w_i \ \partial u_{i-1}} = \bar{k}_{i-(1/2)}\left\{\frac{2}{\Delta} w'_{i-(1/2)}\left[-\frac{1}{\Delta} + \frac{\nu}{2\rho_{i-(1/2)}}\right]\right\} \tag{A19}$$

$$\frac{\partial^2 \Pi_{nl}}{\partial w_i \ \partial u_i} = \bar{k}_{i+(1/2)}\left\{-\frac{2}{\Delta} w'_{i+(1/2)}\left[-\frac{1}{\Delta} + \frac{\nu}{2\rho_{i+(1/2)}}\right]\right\} + \bar{k}_{i-(1/2)}\left\{\frac{2w'_{i-(1/2)}}{\Delta}\left[\frac{1}{\Delta} + \frac{\nu}{2\rho_{i-(1/2)}}\right]\right\} \tag{A20}$$

$$\frac{\partial^2 \Pi_{nl}}{\partial w_i \ \partial u_{i+1}} = \bar{k}_{i+(1/2)}\left\{-\frac{2}{\Delta} w'_{i+(1/2)}\left[\frac{1}{\Delta} + \frac{\nu}{2\rho_{i+(1/2)}}\right]\right\} \tag{A21}$$

where $i = 1, 2, \ldots, N + 1$.

REFERENCES

1. Reissner, Eric: Stresses and Small Displacements of Shallow Spherical Shells. J. Math. Phys.
   I. vol. XXV, no. 1, Feb. 1946, pp. 80-85.
   II. vol. XXV, no. 4, Jan. 1947, pp. 279-300.
2. Kaplan, A.; and Fung, Y. C.: A Nonlinear Theory of Bending and Buckling of Thin Elastic Shallow Spherical Shells. NACA TN 3212, 1954.
3. Archer, Robert R.: Stability Limits for a Clamped Spherical Shell Segment Under Uniform Pressure. Quart. Appl. Math., vol. XV, no. 4, Jan. 1958, pp. 355-366.
4. Reiss, Edward L.; Greenberg, Herbert J.; and Keller, Herbert B.: Nonlinear Deflections of Shallow Spherical Shells. J. Aeron. Sci., vol. 24, no. 7, July 1957, pp. 553-543.
5. Weinitschke, H. J.: On the Nonlinear Theory of Shallow Spherical Shells. J. Soc. Ind. and Appl. Math., vol. 6, no. 3, Sept. 1958, pp. 209-232.
6. Chen, W. L.: Effect of Geometrical Imperfection of the Elastic Buckling of Shallow Spherical Shells. Sc. D. Thesis, Dept. of Civil and Sanitary Engineering, Mass. Inst. of Tech., Jan. 1959.
7. Budiansky, B.: Buckling of Clamped Shallow Spherical Shells. The Theory of Thin Elastic Shells, W. T. Koiter, ed., Interscience Publ., Inc., 1960, pp. 64-94.
8. Thurston, G. A.: A Numerical Solution of the Nonlinear Equations for Axisymmetric Bending of Shallow Spherical Shells. Trans. ASME, Ser. E: J. Appl. Mech., vol. 28, no. 4, Dec. 1961, pp. 557-562.
9. Archer, Robert R.: On the Numerical Solution of the Nonlinear Equations for Shells of Revolution. J. Math. Phys., vol. XLI, 1962, pp. 165-178.
10. Mescall, John F.: Numerical Solutions of the Nonlinear Axisymmetric Equations for Shells of Revolution. AMRA TR 66-11, U.S. Army, May 1966. (Available from DDC as AD 348 418.)
11. Wang, Lean R. L.; Rodriquez-Agrait, Leandro; and Litle, William A.: Effect of Boundary Conditions on Shell Buckling. J. Eng. Mech. Div., Amer. Soc. Civil Eng., vol. 92, no. EM6, Dec. 1966, pp. 101-116.
12. Ritz, Walter: On a New Method of Solving Certain Variational Problems of Mathematical Physics. Transl. No. 1, Counc. Sci. Ind. Res., Div. Aeronaut., Commonwealth of Australia, June 1943.

13. Houbolt, John Cornelius: A Study of Several Aerothermoelastic Problems of Aircraft Structures in High-Speed Flight. Prom. Nr. 2760, Swiss Fed. Inst. Technol. (Zurich), 1958.

14. Walton, William C., Jr.: Application of a General Finite-Difference Method for Calculating Bending Deformations of Solid Plates. NASA TN D-536, 1960.

15. Schaeffer, Harry G.; and Heard, Walter L., Jr.: Evaluation of an Energy Method for Determining Thermal Midplane Stresses in Plates. NASA TN D-2439, 1964.

16. Havner, Kerry S.; and Stanton, Edward L.: On Energy-Derived Difference Equations in Thermal Stress Problems. J. Franklin Inst., vol. 284, no. 2, Aug. 1967, pp. 127-143.

17. Langhaar, Henry L.: Energy Methods in Applied Mechanics. John Wiley & Sons, Inc., c.1962, p. 190.

18. McGill, Robert; and Kenneth, Paul: Solution of Variational Problems by Means of a Generalized Newton-Raphson Operator. AIAA J., vol. 2, no. 10, Oct. 1964, pp. 1761-1766.

19. Cauchy, Augustin: Méthode Génerale Pour la Résolution des Systèmes d'Équations Simultanées. Compt. Rend. Acad. Sci., t.25, 1847, pp. 536-538.

20. Tompkins, Charles B.: Methods of Steep Descent. Modern Mathematics for the Engineer, Edwin F. Beckenbach, ed., McGraw-Hill Book Co., Inc., 1956, pp. 448-479.

21. Beckman, F. S.: The Solution of Linear Equations by the Conjugate Gradient Method. Mathematical Methods for Digital Computers, Vol. I, Anthony Ralston and Herbert S. Wilf, ed., John Wiley & Sons, Inc., c.1960, pp. 62-72.

22. Fletcher, R.; and Reeves, C. M.: Function Minimization by Conjugate Gradients. Computer J., vol. 7, July 1964, pp. 149-154.

23. Hestenes, Magnus R.; and Stiefel, Edward: Methods of Conjugate Gradients for Solving Linear Systems. Res. Paper 2379, J. Res. Nat. Bur. Stand., vol. 49, no. 6, Dec. 1952, pp. 409-436.

24. Fletcher, R.; and Powell, M. J. D.: A Rapidly Convergent Descent Method for Minimization. Computer J., vol. 6, 1963-1964, pp. 163-168.

25. Davidon, William C.: Variable Metric Method for Minimization. ANL-5990 Rev. (Contract W-31-109-eng-38), Argonne Nat. Lab., Nov. 1959.

26. White, Richard N.: Optimum Solution Techniques for Finite-Difference Equations. J. Struct. Div., Amer. Soc. Civil Eng., vol. 89, no. ST4, Aug. 1963, p. 115.

27. Fiacco, Anthony V.; and McCormick, Garth P.: Nonlinear Programming: Sequential Unconstrained Minimization Techniques. John Wiley & Sons, Inc., c.1968.

28. Weinitschke, H. J.: On Asymmetric Buckling of Shallow Spherical Shells. J. Math. Phys., vol. XLIV, no. 1, Mar. 1965, pp. 141-163.

29. Huang, Nai-Chien: Unsymmetrical Buckling of Shallow Spherical Shells. AIAA J. (Tech. Notes Comments), vol. 1, no. 4, Apr. 1963, p. 945.

30. Evensen, David A.; and Fulton, Robert E.: Some Studies on the Nonlinear Dynamic Response of Shell-Type Structures. Dynamic Stability of Structures, George Herrmann, ed., Pergamon Press, Inc., c.1967, pp. 237-254.

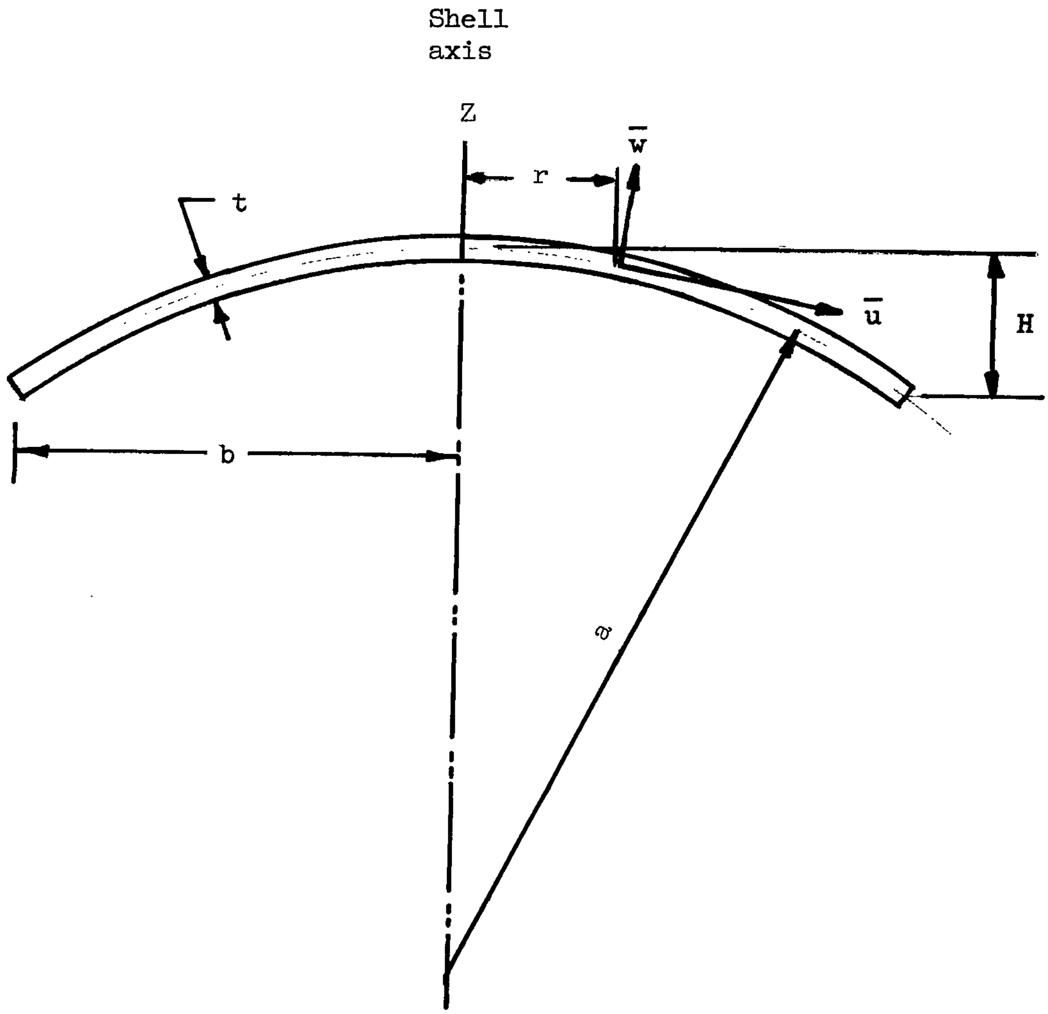

Figure 1.- Cross section of shallow spherical shell.

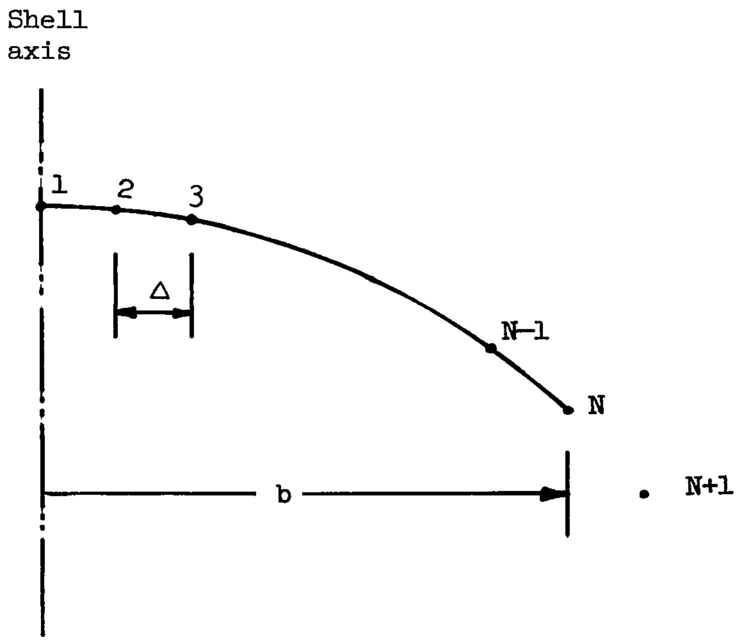

Figure 2.- Meridian of shallow spherical shell showing location of finite-difference stations.

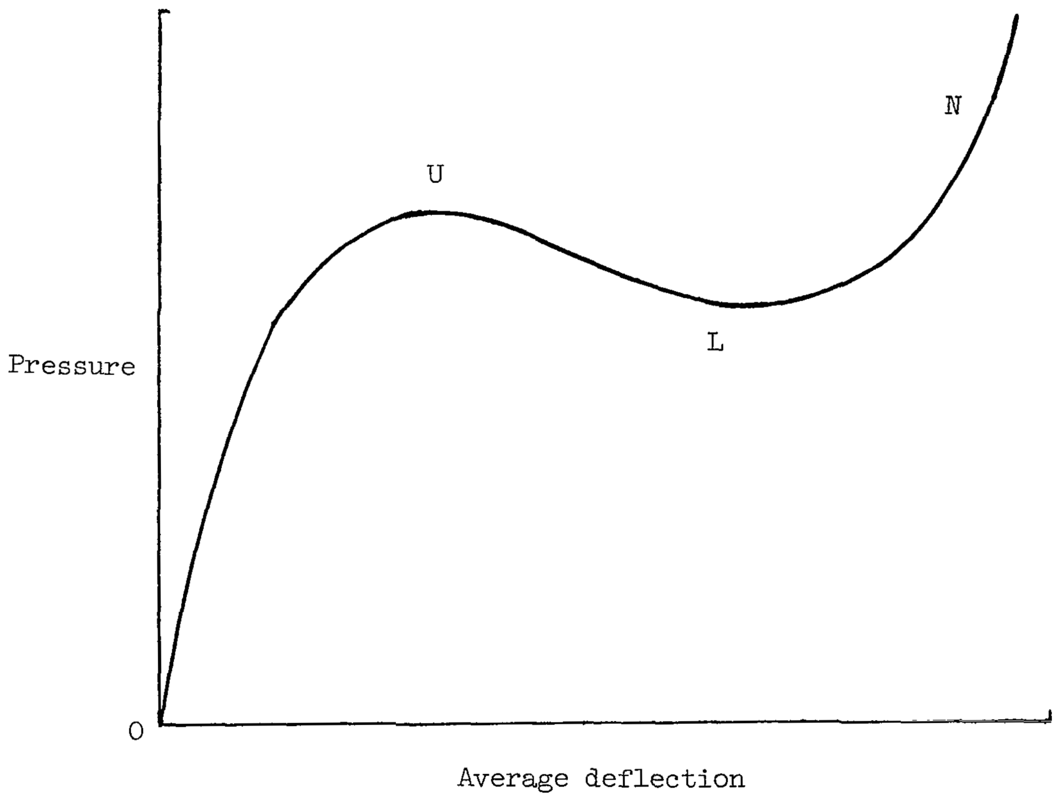

Figure 3.- Typical pressure-deflection curve for a uniformly loaded spherical shell.

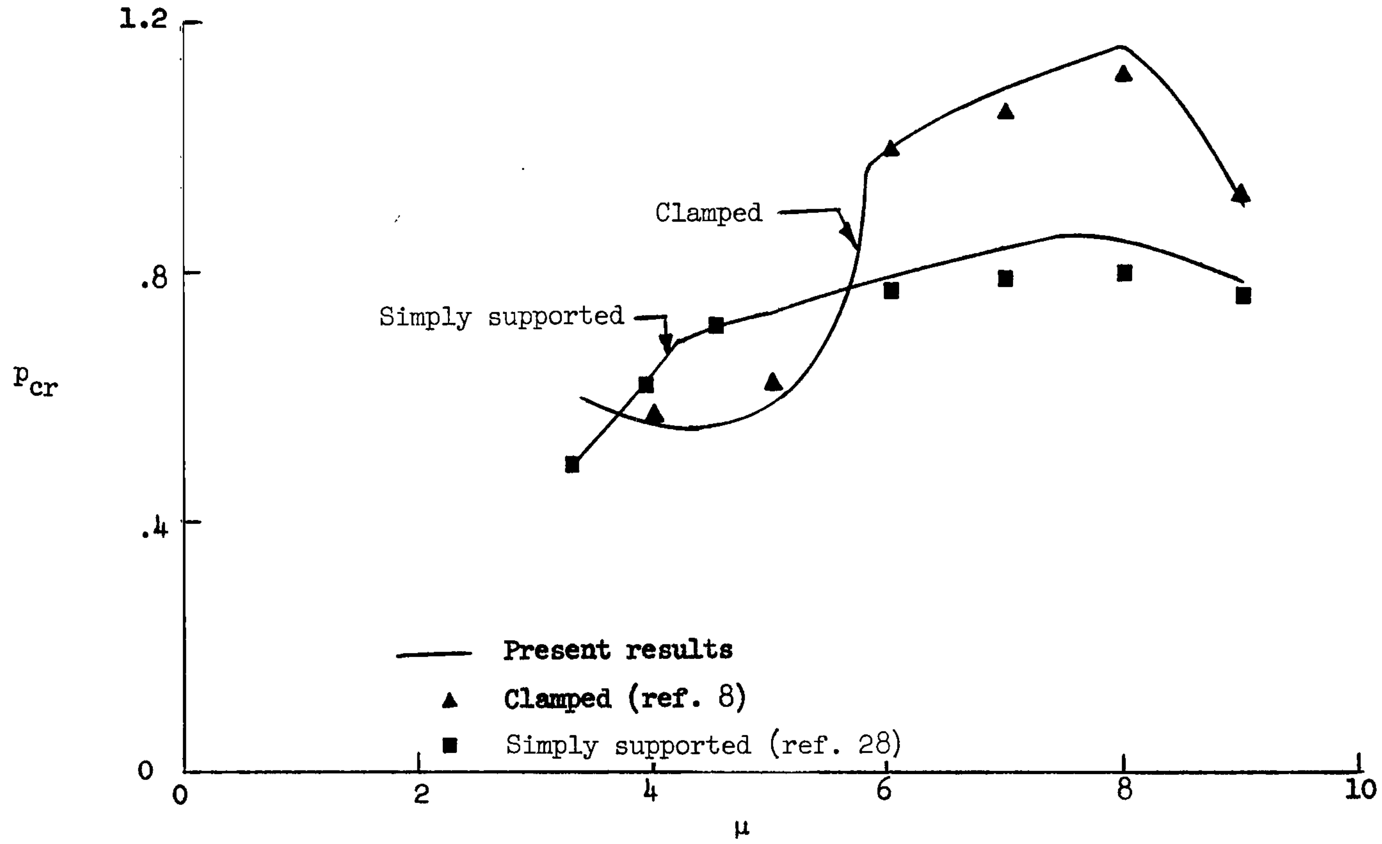

Figure 4.- Axisymmetric buckling pressure p_{cr} as function of shell geometric parameter μ for shallow spherical shell with clamped and simply supported edges.

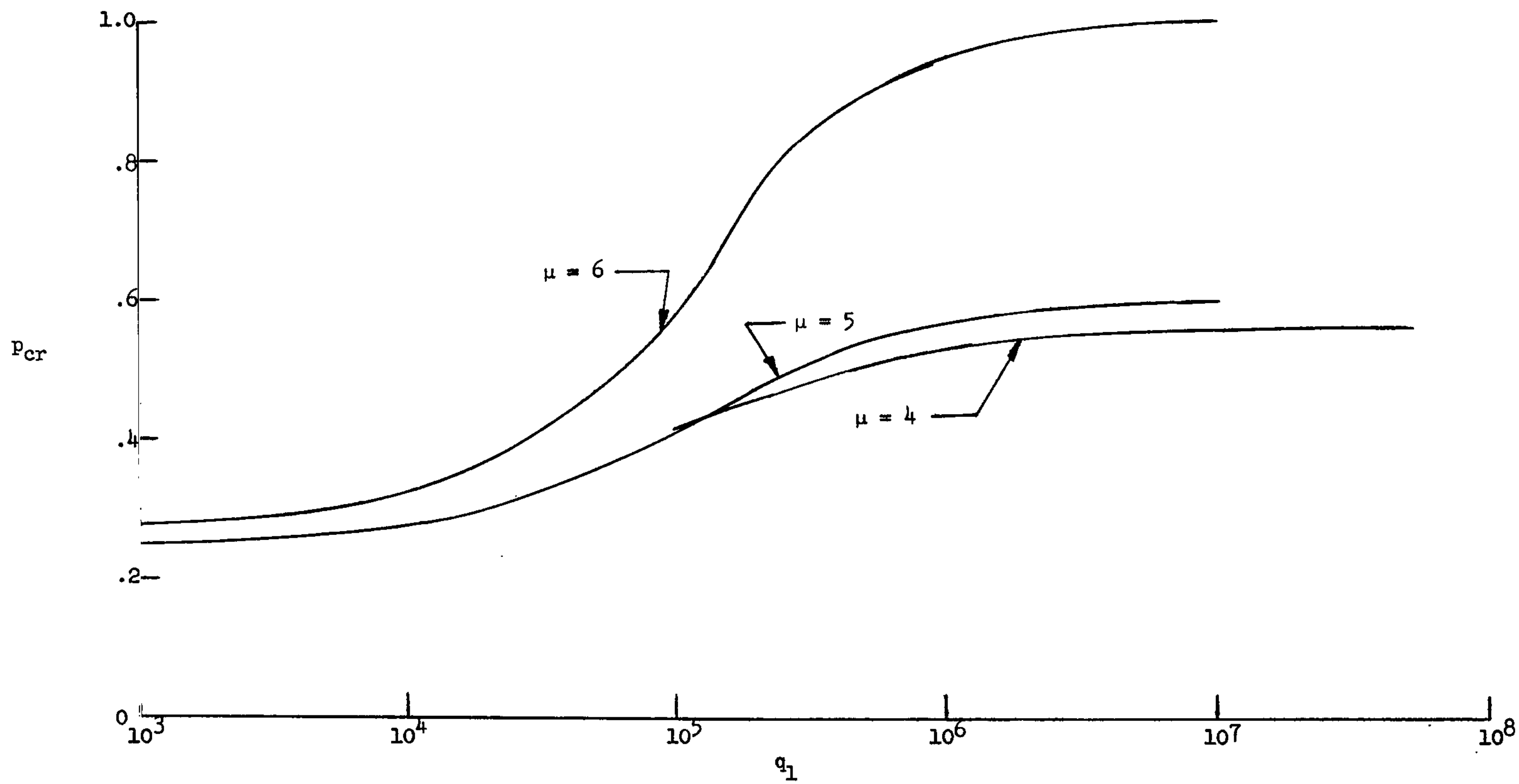

Figure 5.- Axisymmetric buckling pressure p_{cr} as function of in-plane restraint q_1 for various values of geometric shell parameter μ. $q_2 = q_3 = 10^5$.

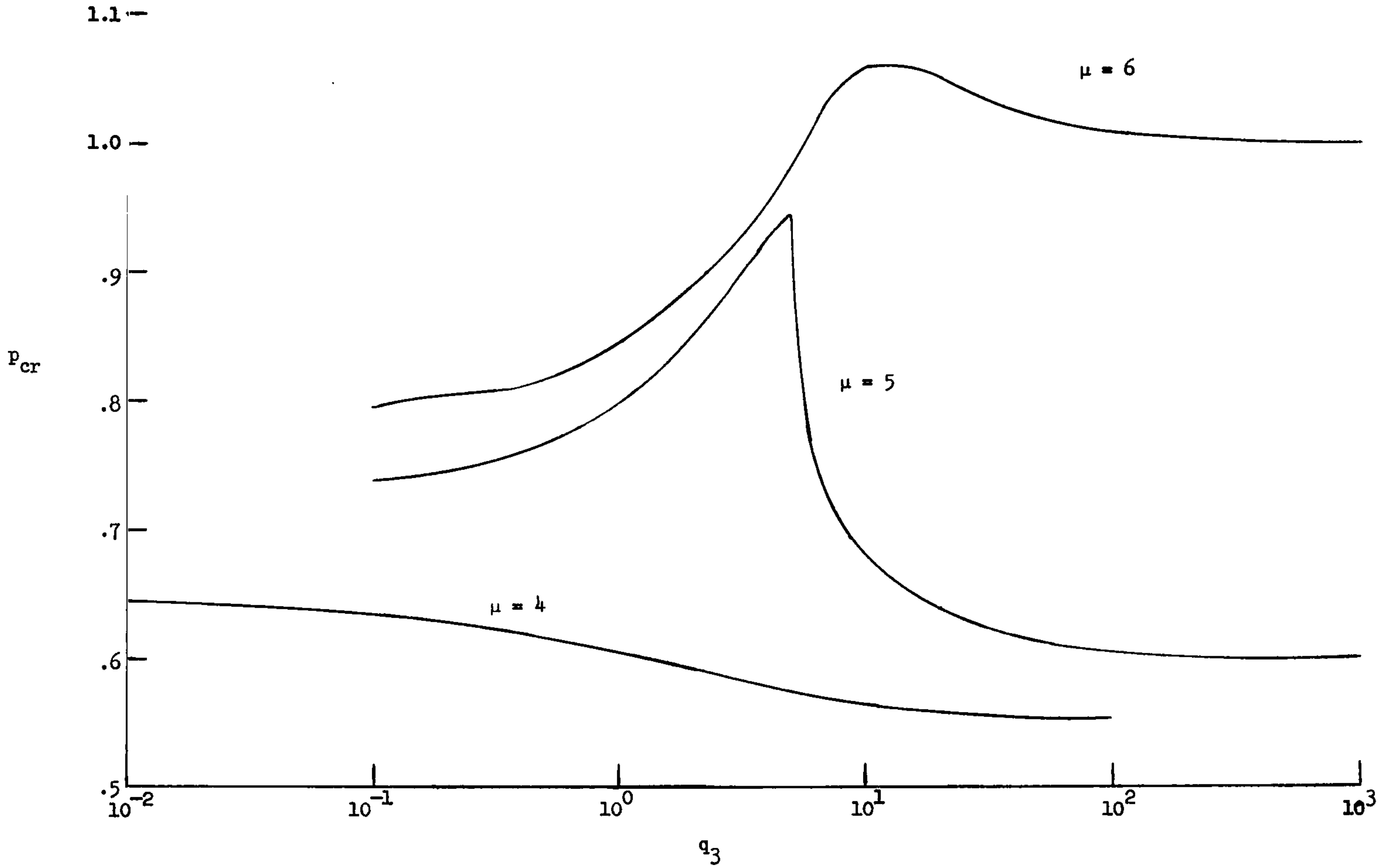

Figure 6.- Axisymmetric buckling pressure p_{cr} as function of rotational restraint q_3 for various values of geometric shell parameter μ. $q_1 = 10^7$; $q_2 = 10^5$.

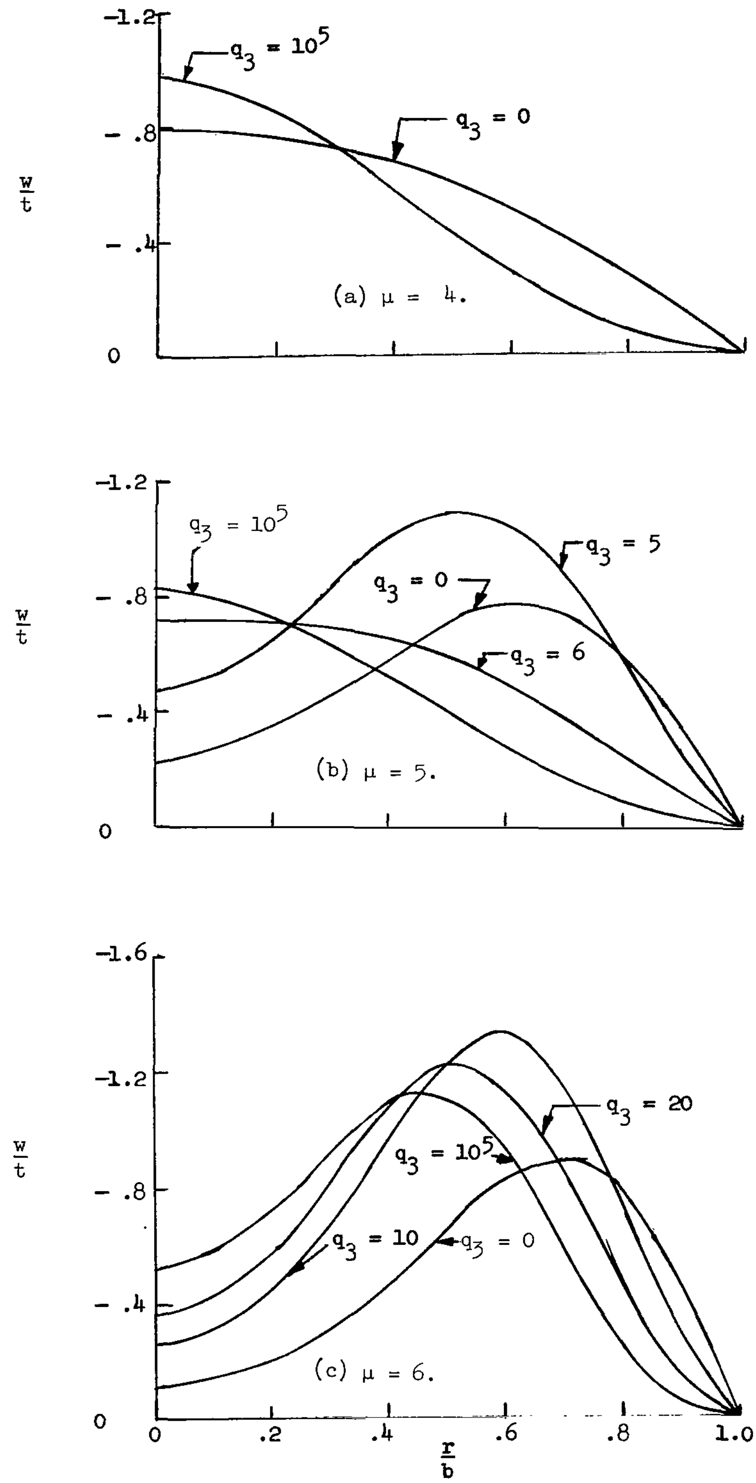

Figure 7.- Normal deflection as function of radial distance for various values of shell parameter μ. $q_1 = 10^7$; $q_2 = 10^5$.

NASA-Langley, 1970 —— 32 L-5959

NATIONAL AERONAUTICS AND SPACE ADMINISTRATION
WASHINGTON, D. C. 20546

OFFICIAL BUSINESS

FIRST CLASS MAIL

POSTAGE AND FEES PAID
NATIONAL AERONAUTICS AND
SPACE ADMINISTRATION

070 001 57 51 30S 70033 00903
AIR FORCE WEAPONS LABORATORY /WLOL/
KIRTLAND AFB, NEW MEXICO 87117

ATT E. LOU BOWMAN, CHIEF, TECH. LIBRARY

POSTMASTER: If Undeliverable (Section 158 Postal Manual) Do Not Return

"The aeronautical and space activities of the United States shall be conducted so as to contribute . . . to the expansion of human knowledge of phenomena in the atmosphere and space. The Administration shall provide for the widest practicable and appropriate dissemination of information concerning its activities and the results thereof."

—NATIONAL AERONAUTICS AND SPACE ACT OF 1958

NASA SCIENTIFIC AND TECHNICAL PUBLICATIONS

TECHNICAL REPORTS: Scientific and technical information considered important, complete, and a lasting contribution to existing knowledge.

TECHNICAL NOTES: Information less broad in scope but nevertheless of importance as a contribution to existing knowledge.

TECHNICAL MEMORANDUMS: Information receiving limited distribution because of preliminary data, security classification, or other reasons.

CONTRACTOR REPORTS: Scientific and technical information generated under a NASA contract or grant and considered an important contribution to existing knowledge.

TECHNICAL TRANSLATIONS: Information published in a foreign language considered to merit NASA distribution in English.

SPECIAL PUBLICATIONS: Information derived from or of value to NASA activities. Publications include conference proceedings, monographs, data compilations, handbooks, sourcebooks, and special bibliographies.

TECHNOLOGY UTILIZATION PUBLICATIONS: Information on technology used by NASA that may be of particular interest in commercial and other non-aerospace applications. Publications include Tech Briefs, Technology Utilization Reports and Notes, and Technology Surveys.

Details on the availability of these publications may be obtained from:

SCIENTIFIC AND TECHNICAL INFORMATION DIVISION
NATIONAL AERONAUTICS AND SPACE ADMINISTRATION
Washington, D.C. 20546